Antibody-based Delivery of TNF to the Tumor Neovasculature Potentiates the Therapeutic Activity of a Peptide Anticancer Vaccine

Originally published in:
Clinical Cancer Research 25(2), https://doi.org/10.1158/1078-0432.CCR-18-1728

Funding acknowledgement:
163479 - Understanding and Exploiting the Molecular Targeting of Tumor Neo-vasculature (SNF)
670603 - Fulfilling Paul Ehrlich's Dream: therapeutics with activation on demand (EC)

Antibody-based delivery of TNF to the tumor neo-vasculature potentiates the therapeutic activity of a peptide anti-cancer vaccine

Philipp Probst[a], Marco Stringhini[a], Danilo Ritz[b], Tim Fugmann[b], Dario Neri[a]*

[a]Department of Chemistry and Applied Biosciences, Swiss Federal Institute of Technology (ETH Zürich), Vladimir-Prelog-Weg 4, CH-8093 Zürich (Switzerland); [b]Philochem AG, Libernstrasse 3, CH-8112 Otelfingen (Switzerland)

Running title: Targeted TNF potentiates the efficacy of a peptide vaccine

Keywords: tumor targeting, TNF, immunotherapy, cancer vaccine, retroviral antigens

Financial Support*:* D. N. gratefully acknowledges ETH Zürich, the Swiss National Science Foundation (Grant Nr. 310030B_163479/1), the ERC Advanced Grant "ZAUBERKUGEL" and the Federal Commission for Technology and Innovation (KTI, Grant Nr. 12803.1 VOUCH-LS) for financial support.

*Corresponding Author
Mailing address: Department of Chemistry and Applied Biosciences
Vladimir-Prelog-Weg 4
CH-8093 Zürich, Switzerland
Telephone number: +41-44-6337401
Fax number: +41-44-6331358
Email address: neri@pharma.ethz.ch

Conflict of interest disclosure: D.N. is co-founder and shareholder of Philogen, a biotech company that owns the F8 antibody. T.F. and D.R. are employees of Philochem AG. The authors have no additional financial interests.

Additional manuscript information: 249 words abstract, 3674 words of text, 7 figures

Submitted to *Cancer Immunology Research* as "Research Article"

Abstract

There is a growing interest in the use of tumor antigens for therapeutic vaccination strategies. Unfortunately, in most cases, the use of peptide vaccines in patients does not mediate shrinkage of solid tumor masses. Here, we studied the opportunity to boost peptide vaccination with F8-TNF, an antibody fusion protein that selectively delivers TNF to the tumor extracellular matrix. In tumor-bearing BALB/c mice, peptide antigens derived from the gp70 envelope protein of the murine leukemia virus exhibited only a modest tumor growth inhibition when used in combination with poly(I:C). However, anti-cancer activity could be substantially increased by combination with F8-TNF. Analysis of T cells in tumor-draining lymph nodes and in the neoplastic mass revealed a dramatic expansion of AH1-specific $CD8^+$ T cells, which were strongly positive for PD-1, LAG-3 and TIM-3. The synergistic anti-cancer activity, observed in the combined use of peptide vaccination and F8-TNF, was largely due to the ability of the fusion protein to induce a rapid hemorrhagic necrosis in the tumor mass, thus leaving few residual tumor cells. While the cell surface phenotype of tumor-infiltrating $CD8^+$ T cells did not substantially change upon treatment, the proportion of AH1-specific T cells was strongly increased in the combination therapy group, reaching more than 50% of the $CD8^+$ T cells within the tumor mass. Since both peptide vaccination strategies and tumor-homing TNF fusion proteins are currently being studied in clinical trials, our study provides a rationale for the combination of these two regimens for the treatment of patients with cancer.

Introduction

Therapeutic cancer vaccination with peptides represents a promising strategy for active immunotherapy, which aims at inducing robust T cell effector functions against neoplastic lesions. However, despite considerable efforts, clinical translation of peptide vaccines into efficacious therapies for cancer patients has been challenging (1,2). Therapeutic immunization with peptides has been evaluated in patients with different types of malignancies including breast cancer, lung cancer, melanoma, pancreatic cancer and colorectal cancer (1). A survival advantage was observed with some vaccines in phase II trials, but objective regressions for solid tumor lesions were rarely reported (1). Recent advances in the understanding of cancer immunology and mechanisms of immune suppression pathways in the tumor microenvironment (TME) have resulted in novel strategies for the application of peptide vaccines with promising results in preclinical *in vivo* studies (3,4). Furthermore, emerging technologies in the discovery of neoantigens from cancer exome sequences have allowed the development of personalized cancer vaccines, which have shown anti-cancer activity in preclinical models and in patients (5-8). However, in order to provoke long-lasting protective anti-tumor immunity with peptide vaccines, suitable combination modalities (which synergistically enhance immunity against tumors, modulate the TME or block immunosuppressive mechanisms) are still needed (1-3).

The gp70 envelope protein of murine leukemia virus (MuLV) represents an attractive antigen for the study of vaccination strategies in immunocompetent mouse models of cancer. The virus is endogenous in the genome of most laboratory mouse strains (9), but MuLV proteins are usually not detected in healthy tissue. Interestingly, strikingly high levels of gp70 have been observed in a large variety of widely used mouse cancer cell lines (10-12). AH1, a peptide derived from the

gp70 envelope protein of the MuLV, was first described by Huang et al. (13) as the major tumor rejection antigen of the BALB/c-derived CT26 colon carcinoma cell line. AH1 has since been used as a model tumor antigen to investigate $CD8^+$ T cell immunity when using CT26 and other mouse tumor models (14-16). Additionally, a number of reports have described the use of AH1 and AH1 related sequences as anti-cancer therapeutics in immunocompetent mouse models of cancer (17-20). Immune responses against endogenous retroviral proteins have been a matter of intense investigations and are not restricted solely to mouse tumor models. Indeed, retroviral sequences have been found in the genome of all vertebrate species (21). Consequently, retroelements of the human endogenous retrovirus (HERV)-K family have shown high expression in human cancers and a potent T cell activity against some retroviral antigens has been observed in cancer patients (22,23).

Among the various antibody therapeutics that could be considered as combination partners for anti-cancer vaccines, we focused our attention on F8-TNF. This non-covalent homotrimeric recombinant protein consists of the scFv(F8) antibody fragment, sequentially fused to murine TNF (24). The F8 antibody (25) recognizes the alternatively-spliced extra-domain A (ED-A) of fibronectin, a target which is virtually undetectable in normal adult tissues (with the exception of the placenta, the endometrium in the proliferative phase and some vessels of the ovaries), while being strongly expressed in the majority of solid tumors (26), lymphomas (27) and in acute leukemias (28,29). After intravenous administration, F8-TNF exhibits an efficient and selective homing to the tumor site, as revealed by quantitative biodistribution studies with radiolabeled protein preparations and by *ex vivo* fluorescence microscopy investigations (12,24). Within the neoplastic mass, F8-TNF can induce a rapid necrosis, turning the tumor into a black, hemorrhagic mass. The therapeutic action of antibody-TNF fusions can be improved by combination with other cytokine-based therapeutics (30-33) or with certain chemotherapeutic agents (12,24,34).

We recently observed that immunocompetent BALB/c mice, bearing subcutaneously-grafted WEHI-164 sarcomas, could be cured by the combined action of F8-TNF and doxorubicin (12,24). Interestingly, cured mice rejected subsequent challenges with WEHI-164 tumors as well as other BALB/c derived tumors (e.g., CT26 and C51 colon carcinomas), in a process that was driven by $CD8^+$ T cells (12). A comparative MHC class I peptidome analysis revealed that AH1 was the immunodominant tumor-rejection antigen in this setting (12).

Encouraged by the anti-cancer activity of F8-TNF used as single agent and by the role played by AH1-specific $CD8^+$ T cells in the tumor rejection process, we decided to investigate combination strategies in immunocompentent mice. Here, we report that peptides derived from the gp70 antigen, displayed only a modest tumor growth inhibition activity, while their action could be substantially enhanced by combination with F8-TNF. A FACS analysis of surface markers (including AH1-specific tetramer reagents) revealed that a large portion of $CD8^+$ T cells within the tumor mass were AH1-specific and had an immunosuppressed/exhausted phenotype. The combination treatment with F8-TNF was effective, as it decreased the bulk of the solid tumor mass, leaving a minimal residual disease that could be attacked by the vaccine-boosted immune system.

Materials and Methods

Animals and tumor models

WEHI-164 fibrosarcoma and CT26 colon carcinoma cells were purchased from the American Type Culture Collection (ATCC). Cells were handled according to the protocols of the supplier and kept in culture for no longer than 2 months. Authentication of the cell lines including check of post-freeze viability, growth properties and morphology, test for mycoplasma contamination, isoenzyme assay and sterility test were performed by the cell bank before shipment. Eight-week-old female BALB/c mice were obtained from Charles River (Germany). All animal experiments were performed under a project license granted by the Veterinäramt des Kantons Zürich, Switzerland (27/2015)

Reagents for therapy experiments

The F8-TNF immunocytokine was produced as described by Hemmerle et al. (24). The AH1 peptide (amino acid sequence: SPSYVYHQF) and the AH1 synthetic long peptide (amino acid sequence: HSPSYVYHQFERRAKYKREPV) were ordered from Biomatik as TFA salts with a purity >98%. Poly(I:C) was obtained from Sigma-Aldrich as lyophilized potassium salt with buffer salts.

AH1 and F8-TNF therapy studies

Exponentially growing WEHI-164 or CT26 tumor cells were harvested, repeatedly washed and resuspended in saline prior to injection. Cells were implanted subcutaneously (s.c.) in the right flank of the mice using $3x10^6$ cells per animal. Tumor volume was calculated as follows: (length [mm] x width [mm] x width [mm])/2. When tumors were clearly palpable, mice were randomly divided into the different treatment groups (n = 5). Vaccination was started when tumor sizes reached about 50 mm^3. Mice were vaccinated s.c. with 50 µg of the peptide in combination with

100 µg poly(I:C) every 4 days. For the AH1 monotherapy study in WEHI-164 bearing mice, control mice were immunized s.c. either with saline alone or with poly(I:C) alone. F8-TNF was injected intravenously (i.v.) in the lateral tail vein. Mice received three injections of either 1 µg F8-TNF (WEHI-164 tumor-bearing mice) or 2.5 µg (CT26 tumor-bearing mice) every 48 h starting on the day after vaccination. For combination studies of the peptide vaccines with F8-TNF, mice were grouped as follows: control group (received 100 µg poly(I:C) s.c. and saline i.v.), AH1 vaccine group (peptide vaccine s.c. and saline i.v.), F8-TNF group (100 µg poly(I:C) s.c. and F8-TNF i.v.) and combo group (peptide vaccine s.c. and F8-TNF i.v.). Animals were euthanized when tumor volumes reached a maximum of 2000 mm^3 or weight loss exceeded 15%.

Affinity purification of mouse MHC I molecules

Affinity purification of murine MHC I complexes was performed as recently described (12). Lysis of CT26 tumor cells was performed at a density of approximately $2.5x10^7$ cells/mL. M1/42 (BioXcell) antibody-coupled resin was used for the purification of MHC I complexes from the cell lysates.

Analysis of MHC I peptides by liquid chromatography-mass spectrometry

Analysis of MHC I peptides by liquid chromatography-mass spectrometry (LC-MS) was performed as previously described for human HLA class I peptides by Gloger et al. (35). The datasets were searched using the MaxQuant software (36) against all murine proteins (89'527 entries) of the UniProt database, downloaded on the 22nd March 2018. MaxQuant parameters were essentially set as described (35): (1) digestion mode: unspecific, (2) first search mass tolerance 20 ppm; main search mass tolerance 4.5 ppm, (3) fragment mass tolerance 20 ppm, (4) one variable modification: oxidation of methionine, (5) no specific amino acids for the generation of the decoy databases, (6) peptide false discovery rate (FDR) 1 %, protein FDR 1 %, (7) peptide length allowed: 8–20 amino acids. Match between runs was allowed with a matching time window of 3

min and an alignment time window of 20 min. Reverse hits were removed from the "peptide.txt" output file. For comparison reasons, WEHI-164 samples from (12) were reanalyzed with the same parameters. The Maxquant output tables can be found in **Supplementary Table 1**.

Gibbs clustering of MHC class I peptides and annotation of clusters to MHC

All 9mers of the CT26 MHC class I peptidome were analyzed by the GibbsCluster-2.0 Server (37) using the default settings without alignment. Based on the resulting clusters, the peptides were annotated to the murine MHC class I alleles H2-D^d, -K^d, and -L^d.

CD4 epitope predictions of the gp70 envelope protein

CD4 epitope prediction was based on the peptide binding prediction presented previously (38). In brief, the gp70 protein sequence (UniProt accession: Q61919) was cut into all possible 9mers and scored with position-specific scoring matrices from (39). The higher the binding score, the higher the possibility for a given peptide to bind to a given MHC class II complex. All 9mers with a score greater than 6 are presented in **Supplementary Table 2**. These peptide sequences typically can bind to MHC class II complexes. The 21mer for vaccination was designed to contain the AH1 peptide and three of the four highest scoring peptide sequences.

Generation of AH1 tetramers

Expression of recombinant murine MHC class I H-$2L^d$ heavy chain and of human β2-microglobulin was performed according to established protocols. Refolding of the MHC class I complex with the AH1 peptide was followed by biotinylation with MBP-BirA and size exclusion chromatography (Superdex S75 10/300 GL, GE Healthcare). Assembled monomers were stored in 16% glycerol at -20 ºC. MHC class I tetramers were produced by addition of APC-conjugated streptavidin (Biolegend) to the monomers at a final molecular ratio of 4:1. Plasmids of the H-$2L^d$

heavy chain and of human β2-microglobulin were a kind gift of Prof. A. Oxenius (ETH Zürich, Switzerland). The AH1 (SPSYVYHQF) peptide was ordered from Biomatik.

Sample preparation for flow cytometry

CT26 or WEHI-164 tumor-bearing mice were vaccinated as described above. The injection of F8-TNF was postponed by 4 days, in order to ensure an adequate tumor size for the analysis of tumor infiltrating lymphocytes. Tumor draining lymph nodes (DLN) and tumors were excised on the day after the first F8-TNF injection. DLN were minced in PBS, treated RBC Lysis Buffer (Biolegend), passed through a 40 µm cell-strainer (EASYstrainer, greiner bio-one) and repeatedly washed. The single cell suspension was used directly for flow cytometric analyses. Tumors were cut into small pieces and digested in RPMI-1640 (Thermo Fisher, with L-glutamine) containing antibiotic-antimycotic solution (Thermo Fisher), 1 mg/mL collagenase II (Thermo Fisher) and 0.1 mg/mL DNase I (Roche) at 37ºC, 5% CO_2 for 2 h in an orbital shaker set to 110 rpm. The cell suspension was then passed through a 40 µm cell-strainer (EASYstrainer, greiner bio-one), repeatedly washed and immediately used for flow cytometric analyses.

Flow cytometric analyses

Approximately $1*10^6$ cells from DLN or $5*10^6$ cells from tumors were stained for 30 min at room temperature with Zombie Red Fixable Viability Kit (Biolegend) and afterwards incubated on ice for 20 min with TruStain fcX (anti-mouse CD16/32, Biolegend). Surface staining was performed with APC-coupled AH1 tetramers and fluorochrome-conjugated antibodies against Thy1.2 (clone 53-2.1), CD8 (53-6.7), CD4 (GK1.5), CD44 (IM7), CD62L (MEL-14), PD-1 (29F.1A12), TIM-3 (RMT3-23) and LAG-3 (C9B7W), which were all purchased from Biolegend. Cells were stained in PBS containing 0.5% bovine serum albumin (BSA) and 2 mM EDTA for 1 h at 4ºC. For the staining of intracellular markers, cells were fixed and permeabilized using the eBioscience Foxp3

/ Transcription Factor Staining Buffer Set according to the protocol of the manufacturer. Cells were incubated with fluorochrome-conjugated antibodies against Ki-67 (16A8, Biolegend) and Foxp3 (MF-14, Biolegend) in PBS containing 0.5% BSA and 2 mM EDTA for 30 min at room temperature. Cells were analyzed on a CytoFLEX cytometer (Beckman Coulter) and data were processed using FlowJo (v.10, Tree Star).

Statistical analyses

Data was analyzed using Prism 7.0 (GraphPad Software, Inc.). Statistical significances were determined with a regular two-way ANOVA test with the Bonferroni post-test. A Student's *t* test was used to assess the differences of the effector-to-tumor cell ratios between the different treatment groups. Data represent means ± SEM. $P < 0.05$ was considered statistically significant. * = $p < 0.05$, ** = $p < 0.01$, *** $p = < 0.001$, **** = $p < 0.0001$.

Results

Therapy experiments with therapeutic peptide vaccines

In a first experiment, we studied the tumor growth inhibition activity of AH1 (amino acid sequence: SPSYVYHQF), following subcutaneous administration to immunocompetent BALB/c mice, bearing established WEHI-164 sarcomas of approximately 50 mm^3 in size [**Figure 1A**]. The peptide, which was given at a dose of 50 µg in combination with 100 µg poly(I:C), did not stabilize the size of the neoplastic mass, but delayed tumor growth significantly more compared to the adjuvant alone or saline ($p < 0.0001$). When the experiment was repeated, including treatment groups with a suboptimal dose of F8-TNF (1 µg; sarcomas are very sensitive to the action of TNF) (12,24), a potentiation of anti-cancer activity was observed, with 3/6 cured mice in the combination group [**Figure 1B**]. Similar investigations were performed in mice bearing subcutaneous CT26 adenocarcinomas. Also in this case, with a full dose of F8-TNF (2.5 µg), cancer cures were observed in the combination group (3/5 mice) [**Figure 1D**]. In an attempt to boost the anti-cancer activity of the AH1 peptide, we used a synthetic long peptide (SLP) of the natural gp70 amino acid sequence, which contains AH1 and three putative H2 $I\text{-}E^d$ epitopes (amino acid sequence: HSPSYVYHQFERRAKYKREPV, **Supplementary Table 2**). However, the inclusion of the additional epitope did not improve therapeutic performance [**Figure 1D**].

MHC class I peptidome analysis

We had previously reported that the AH1 peptide is efficiently presented on MHC class I molecules in WEHI-164 tumors (12). Here, we have investigated if the MHC peptidome of CT26 tumor cells is comparable with the WEHI-164 peptidome. MHC class I peptidome analysis from five replicates of 100 million cultured CT26 tumor cells led to the identification of a total of 1869 sequences [**Figure 2A**] with the majority of eluted peptides being nine amino acids in length [**Figure 2B**]. A comparison of the WEHI-164 peptidome with the CT26 peptidome showed that

38.5% of all peptide sequences were shared between the two cell lines [**Figure 2C**]. Among the shared peptides was also the AH1 peptide sequence [**Supplementary Table 1**]. A GibbsCluster analysis further revealed that 693, 585, and 552 peptides were eluted from H2-D^d, -K^d and -L^d alleles [**Figure 2D**].

Mechanistic investigations

In order to gain mechanistic insights into the anti-cancer activity in the various treatment groups, we compared the density of T cells in draining lymph nodes and in the tumors of CT26-bearing mice. The highest density of $CD8^+$ T cells could be observed in specimens derived from the combination therapy group ($p = 0.0182$, compared to the control group in DLN). Moreover, $CD8^+$ T cells were more abundant than $CD4^+$ T cells within all neoplastic masses [**Figure 3A**]. A slight elevation in the relative frequency of Foxp3-positive T cells was observed in all treatment groups, which had received the AH1 peptide [**Figure 3B**].

FACS analysis, performed with a fluorescently-labeled AH1-specific tetramer reagent, revealed that AH1-specific $CD8^+$ T cells increased in draining lymph nodes of mice with tumor (0.5%), relative to naïve mice (not detectable) [**Figure 4A and Supplementary Figure 1**]. Treatment with F8-TNF (alone or in combination with AH1 peptide) mediated a further increase in AH1-specific T cells (to 1.2% and 1.4%, respectively) [**Figure 4A**]. The frequency of AH1-specific $CD8^+$ T cells increased substantially within the solid tumor mass, reaching 15.9% of all T cells in the combination treatment group [**Figure 4B**]. In this setting, 51% of all $CD8^+$ T cells in the tumor were specific to AH1, a proportion that was substantially greater than in mice, which had received only saline plus poly(I:C) (29%) [**Figure 4C**].

Furthermore, we observed that most $CD4^+$ and $CD8^+$ T cells were naïve ($CD44^{low}$, approx. 80-90%) in tumor draining lymph nodes. However, AH1-specific $CD8^+$ T cells had an effector phe-

notype ($CD44^{high}$, >75%) suggesting a possible role in tumor surveillance [**Figure 5A,B**]. Interestingly, these AH1-specific T cells were positive for the exhaustion markers PD-1, LAG-3 and (to a lesser extent) TIM-3 [**Figure 5C**]. There were no striking differences among treatment groups, even though mice that had received AH1 (alone or in combination) showed an increased proliferation (Ki-67 staining) [**Figure 5C**]. A similar analysis was performed for tumor-infiltrating T cells. An effector phenotype was observed for both $CD4^+$ and $CD8^+$ T cells, the latter exhibiting a higher expression of inhibitory surface markers [**Figure 6**].

F8-TNF treatment leads to a rapid hemorrhagic necrosis for large portions of the solid tumor mass. This is reflected not only in a FACS analysis of cellular contents of neoplastic masses from the various treatment groups [**Figure 7A**], but also in a macroscopic inspection of black scab formation [**Figure 7B**] as well as in H&E staining of tumor sections following treatment [**Figure 7C**]. In this context, the immune system has to deal with minimal residual disease and it is reasonable to assume that the effects of AH1 vaccination are more efficacious when a smaller number of tumor cells needs to be killed. The vaccination regimen further increased the effector-to-tumor cell ratios by boosting the AH1-specific $CD8^+$ T cells [**Figure 7D**].

Discussion

In this study, we have shown that the AH1 peptide is the main target of $CD8^+$ T cell recognition for two types of tumors (CT26 and WEHI-164) grown in BALB/c mice. The use of the AH1 peptide as therapeutic vaccine led only to a modest tumor growth retardation when used as monotherapy, whereas this interventional modality could be boosted by combination with F8-TNF.

The role of AH1 as a tumor-rejection antigen in BALB/c mice has been extensively studied (13,16-20). We have recently reported that mice cured from WEHI-164 sarcomas would reject subsequent challenges with the same tumor cells or with different BALB/c-derived tumor cell lines (12). However, F1F tumors (which are low in gp70 envelope protein of MuLV) were not rejected, thus providing additional evidence for the dominant role of AH1 recognition in tumor surveillance.

The experiments presented in this paper suggest that the targeted delivery of TNF may be attractive for the boosting of therapeutic anti-cancer peptide vaccination strategies. The fusion protein L19-TNF (34), closely related to F8-TNF, is currently being studied in Phase III clinical trials for the treatment of metastatic soft-tissue sarcoma, in combination with doxorubicin (Eudra-CT no. 2012-105 000950-75) (33,40,41). While the F8 antibody recognizes the ED-A domain of fibronectin, L19 is specific to the alternatively-spliced ED-B domain of fibronectin (42). In mice, the two antibodies display a similar tumor-targeting performance. NGR-TNF is a second TNF-based biopharmaceutical, featuring an NGR-containing peptide at the N-terminus of the TNF moiety (43). This peptide recognizes a CD13 aminopeptidase variant, which is often associated with the tumor neo-vasculature (44,45). NGR-TNF is currently being tested in a Phase III trial in patients with malignant pleural mesothelioma, as well as in randomized Phase II trials in four different types of solid tumors, either as monotherapy or in combination with chemotherapeutic agents.

AH1-specific $CD8^+$ T cells display an immunosuppressed/exhauseted phenotype in the various treatment groups presented in this study [**Figures 5** and **6**]. Similar phenotypes were observed in neoantigen-specific lymphocytes in the peripheral blood of melanoma patients, on tumor antigen-specific $CD8^+$ T cells induced by melanoma vaccines in patients (46,47), as well as in tumor-infiltrating T cells for other malignancies (e.g., (48)). It is reasonable to assume that a combination with immune check-point inhibitors may further boost therapeutic peptide vaccination (1-3). A combination of peptide vaccination with PD-1-blockade and an engineered cytokine (IL2-Fc) has recently been reported to cure different mouse models of cancer (4).

F8-TNF is likely to mediate a potent anti-cancer effect by triggering a rapid hemorrhagic necrosis within the tumor mass. The advent of perfusion MRI methodologies appears to be ideally suited in order to assess whether a similar process may be used to fight cancer in patients. Demonstration of this pharmacodynamic effect in clinical trials would provide a strong rationale for the combination of TNF-based biopharmaceuticals with anti-cancer vaccines.

Acknowledgements

Financial support by the ETH Zürich, the Swiss National Science Foundation, the ERC Advanced Grant “ZAUBERKUGEL” and the Federal Commission for Technology and Innovation is gratefully acknowledged.

References

1. Melero I, Gaudernack G, Gerritsen W, Huber C, Parmiani G, Scholl S, *et al.* Therapeutic vaccines for cancer: an overview of clinical trials. Nature Reviews Clinical Oncology 2014;11:509.
2. Guo C, Manjili MH, Subjeck JR, Sarkar D, Fisher PB, Wang X-Y. Therapeutic Cancer Vaccines: Past, Present, and Future. In: Tew KD, Fisher PB, editors. Adv Cancer Res. Volume 119: Academic Press; 2013. p 421-75.
3. Melief CJM, van Hall T, Arens R, Ossendorp F, van der Burg SH. Therapeutic cancer vaccines. The Journal of Clinical Investigation 2015;125(9):3401-12.
4. Moynihan KD, Opel CF, Szeto GL, Tzeng A, Zhu EF, Engreitz JM, *et al.* Eradication of large established tumors in mice by combination immunotherapy that engages innate and adaptive immune responses. Nat Med 2016;22:1402.
5. Gubin MM, Zhang X, Schuster H, Caron E, Ward JP, Noguchi T, *et al.* Checkpoint blockade cancer immunotherapy targets tumour-specific mutant antigens. Nature 2014;515:577.
6. Ott PA, Hu Z, Keskin DB, Shukla SA, Sun J, Bozym DJ, *et al.* An immunogenic personal neoantigen vaccine for patients with melanoma. Nature 2017;547:217.
7. Sahin U, Derhovanessian E, Miller M, Kloke B-P, Simon P, Löwer M, *et al.* Personalized RNA mutanome vaccines mobilize poly-specific therapeutic immunity against cancer. Nature 2017;547:222.
8. Carreno BM, Magrini V, Becker-Hapak M, Kaabinejadian S, Hundal J, Petti AA, *et al.* A dendritic cell vaccine increases the breadth and diversity of melanoma neoantigen-specific T cells. Science (New York, NY) 2015;348(6236):803-8.
9. Jenkins NA, Copeland NG, Taylor BA, Lee BK. Organization, distribution, and stability of endogenous ecotropic murine leukemia virus DNA sequences in chromosomes of Mus musculus. J Virol 1982;43(1):26-36.
10. Scrimieri F, Askew D, Corn DJ, Eid S, Bobanga ID, Bjelac JA, *et al.* Murine leukemia virus envelope gp70 is a shared biomarker for the high-sensitivity quantification of murine tumor burden. Oncoimmunology 2013;2(11):e26889.
11. Castle JC, Loewer M, Boegel S, de Graaf J, Bender C, Tadmor AD, *et al.* Immunomic, genomic and transcriptomic characterization of CT26 colorectal carcinoma. BMC Genomics 2014;15(1):190.
12. Probst P, Kopp J, Oxenius A, Colombo MP, Ritz D, Fugmann T, *et al.* Sarcoma Eradication by Doxorubicin and Targeted TNF Relies upon CD8+ T-cell Recognition of a Retroviral Antigen. Cancer Res 2017;77(13):3644-54.
13. Huang AY, Gulden PH, Woods AS, Thomas MC, Tong CD, Wang W, *et al.* The immunodominant major histocompatibility complex class I-restricted antigen of a murine colon tumor derives from an endogenous retroviral gene product. Proc Natl Acad Sci USA 1996;93(18):9730-5.
14. James E, Yeh A, King C, Korangy F, Bailey I, Boulanger DS, *et al.* Differential Suppression of Tumor-Specific CD8+ T Cells by Regulatory T Cells. The Journal of Immunology 2010;185(9):5048-55.
15. Wang S, Campos J, Gallotta M, Gong M, Crain C, Naik E, *et al.* Intratumoral injection of a CpG oligonucleotide reverts resistance to PD-1 blockade by expanding multifunctional CD8(+) T cells. Proceedings of the National Academy of Sciences of the United States of America 2016;113(46):E7240-E9.
16. Miller CT, Graham LJ, Bear HD. Adoptive immunotherapy (AIT) of established tumors with tumor antigen peptide-sensitized T cells. Cancer Res 2004;64(7 Supplement):1264-.

17. Slansky JE, Rattis FM, Boyd LF, Fahmy T, Jaffee EM, Schneck JP, *et al.* Enhanced antigen-specific antitumor immunity with altered peptide ligands that stabilize the MHC-peptide-TCR complex. Immunity 2000;13(4):529-38.
18. Jordan KR, McMahan RH, Kemmler CB, Kappler JW, Slansky JE. Peptide vaccines prevent tumor growth by activating T cells that respond to native tumor antigens. Proc Natl Acad Sci USA 2010;107.
19. Kershaw MH, Hsu C, Mondesire W, Parker LL, Wang G, Overwijk WW, *et al.* Immunization against endogenous retroviral tumor-associated antigens. Cancer Res 2001;61(21):7920-4.
20. Casares N, Lasarte JJ, Cerio ALDd, Sarobe P, Ruiz M, Melero I, *et al.* Immunization with a tumor - associated CTL epitope plus a tumor - related or unrelated Th1 helper peptide elicits protective CTL immunity. Eur J Immunol 2001;31(6):1780-9.
21. Kassiotis G, Stoye JP. Immune responses to endogenous retroelements: taking the bad with the good. Nat Rev Immunol 2016;16(4):207-19.
22. Kassiotis G. Endogenous Retroviruses and the Development of Cancer. The Journal of Immunology 2014;192(4):1343-9.
23. Schiavetti F, Thonnard J, Colau D, Boon T, Coulie PG. A human endogenous retroviral sequence encoding an antigen recognized on melanoma by cytolytic T lymphocytes. Cancer Res 2002;62(19):5510-6.
24. Hemmerle T, Probst P, Giovannoni L, Green AJ, Meyer T, Neri D. The antibody-based targeted delivery of TNF in combination with doxorubicin eradicates sarcomas in mice and confers protective immunity. Br J Cancer 2013;109(5):1206-13.
25. Villa A, Trachsel E, Kaspar M, Schliemann C, Sommavilla R, Rybak J-N, *et al.* A high-affinity human monoclonal antibody specific to the alternatively spliced EDA domain of fibronectin efficiently targets tumor neo-vasculature in vivo. Int J Cancer 2008;122(11):2405-13.
26. Rybak JN, Roesli C, Kaspar M, Villa A, Neri D. The extra-domain A of fibronectin is a vascular marker of solid tumors and metastases. Cancer Res 2007;67(22):10948-57.
27. Schliemann C, Wiedmer A, Pedretti M, Szczepanowski M, Klapper W, Neri D. Three clinical-stage tumor targeting antibodies reveal differential expression of oncofetal fibronectin and tenascin-C isoforms in human lymphoma. Leukemia Res 2009;33(12):1718-22.
28. Gutbrodt KL, Schliemann C, Giovannoni L, Frey K, Pabst T, Klapper W, *et al.* Antibody-based delivery of interleukin-2 to neovasculature has potent activity against acute myeloid leukemia. Sci Transl Med 2013;5(201):201ra118.
29. Schliemann C, Gutbrodt KL, Kerkhoff A, Pohlen M, Wiebe S, Silling G, *et al.* Targeting Interleukin-2 to the Bone Marrow Stroma for Therapy of Acute Myeloid Leukemia Relapsing after Allogeneic Hematopoietic Stem Cell Transplantation. Cancer Immunology Research 2015;3(5):547-56.
30. Halin C, Gafner V, Villani ME, Borsi L, Berndt A, Kosmehl H, *et al.* Synergistic therapeutic effects of a tumor targeting antibody fragment, fused to interleukin 12 and to tumor necrosis factor alpha. Cancer Res 2003;63(12):3202-10.
31. Balza E, Carnemolla B, Mortara L, Castellani P, Soncini D, Accolla RS, *et al.* Therapy-induced antitumor vaccination in neuroblastomas by the combined targeting of IL-2 and TNFalpha. Int J Cancer 2010;127(1):101-10.
32. Schwager K, Hemmerle T, Aebischer D, Neri D. The immunocytokine L19-IL2 eradicates cancer when used in combination with CTLA-4 blockade or with L19-TNF. J Invest Dermatol 2013;133(3):751-8.

33. Danielli R, Patuzzo R, Di Giacomo AM, Gallino G, Maurichi A, Di Florio A, *et al.* Intralesional administration of L19-IL2/L19-TNF in stage III or stage IVM1a melanoma patients: results of a phase II study. Cancer Immunol, Immunother 2015;64(8):999-1009.
34. Borsi L, Balza E, Carnemolla B, Sassi F, Castellani P, Berndt A, *et al.* Selective targeted delivery of TNFalpha to tumor blood vessels. Blood 2003;102(13):4384-92.
35. Gloger A, Ritz D, Fugmann T, Neri D. Mass spectrometric analysis of the HLA class I peptidome of melanoma cell lines as a promising tool for the identification of putative tumor-associated HLA epitopes. Cancer Immunol, Immunother 2016:1-17.
36. Cox J, Mann M. MaxQuant enables high peptide identification rates, individualized p.p.b.-range mass accuracies and proteome-wide protein quantification. Nat Biotech 2008;26(12):1367-72.
37. Andreatta M, Alvarez B, Nielsen M. GibbsCluster: unsupervised clustering and alignment of peptide sequences. Nucleic Acids Res 2017;45(W1):W458-W63.
38. Fugmann T, Sofron A, Ritz D, Bootz F, Neri D. The MHC Class II Immunopeptidome of Lymph Nodes in Health and in Chemically Induced Colitis. The Journal of Immunology 2017;198(3):1357-64.
39. Sofron A, Ritz D, Neri D, Fugmann T. High - resolution analysis of the murine MHC class II immunopeptidome. Eur J Immunol 2016;46(2):319-28.
40. Spitaleri G, Berardi R, Pierantoni C, De Pas T, Noberasco C, Libbra C, *et al.* Phase I/II study of the tumour-targeting human monoclonal antibody-cytokine fusion protein L19-TNF in patients with advanced solid tumours. J Cancer Res Clin Oncol 2013;139(3):447-55.
41. Papadia F, Basso V, Patuzzo R, Maurichi A, Di Florio A, Zardi L, *et al.* Isolated limb perfusion with the tumor-targeting human monoclonal antibody-cytokine fusion protein L19-TNF plus melphalan and mild hyperthermia in patients with locally advanced extremity melanoma. J Surg Oncol 2013;107(2):173-9.
42. Neri D, Bicknell R. Tumour vascular targeting. Nat Rev Cancer 2005;5(6):436-46.
43. Curnis F, Sacchi A, Borgna L, Magni F, Gasparri A, Corti A. Enhancement of tumor necrosis factor α antitumor immunotherapeutic properties by targeted delivery to aminopeptidase N (CD13). Nat Biotechnol 2000;18:1185.
44. Pasqualini R, Koivunen E, Kain R, Lahdenranta J, Sakamoto M, Stryhn A, *et al.* Aminopeptidase N Is a Receptor for Tumor-homing Peptides and a Target for Inhibiting Angiogenesis. Cancer Res 2000;60(3):722-7.
45. Corti A, Curnis F, Arap W, Pasqualini R. The neovasculature homing motif NGR: more than meets the eye. Blood 2008;112(7):2628-35.
46. Gros A, Parkhurst MR, Tran E, Pasetto A, Robbins PF, Ilyas S, *et al.* Prospective identification of neoantigen-specific lymphocytes in the peripheral blood of melanoma patients. Nat Med 2016;22:433.
47. Fourcade J, Sun Z, Pagliano O, Chauvin J-M, Sander C, Janjic B, *et al.* PD-1 and Tim-3 regulate the expansion of tumor antigen-specific CD8+ T cells induced by melanoma vaccines. Cancer Res 2014;74(4):1045-55.
48. Bobisse S, Genolet R, Roberti A, Tanyi JL, Racle J, Stevenson BJ, *et al.* Sensitive and frequent identification of high avidity neo-epitope specific CD8 + T cells in immunotherapy-naive ovarian cancer. Nature Communications 2018;9(1):1092.

Figures

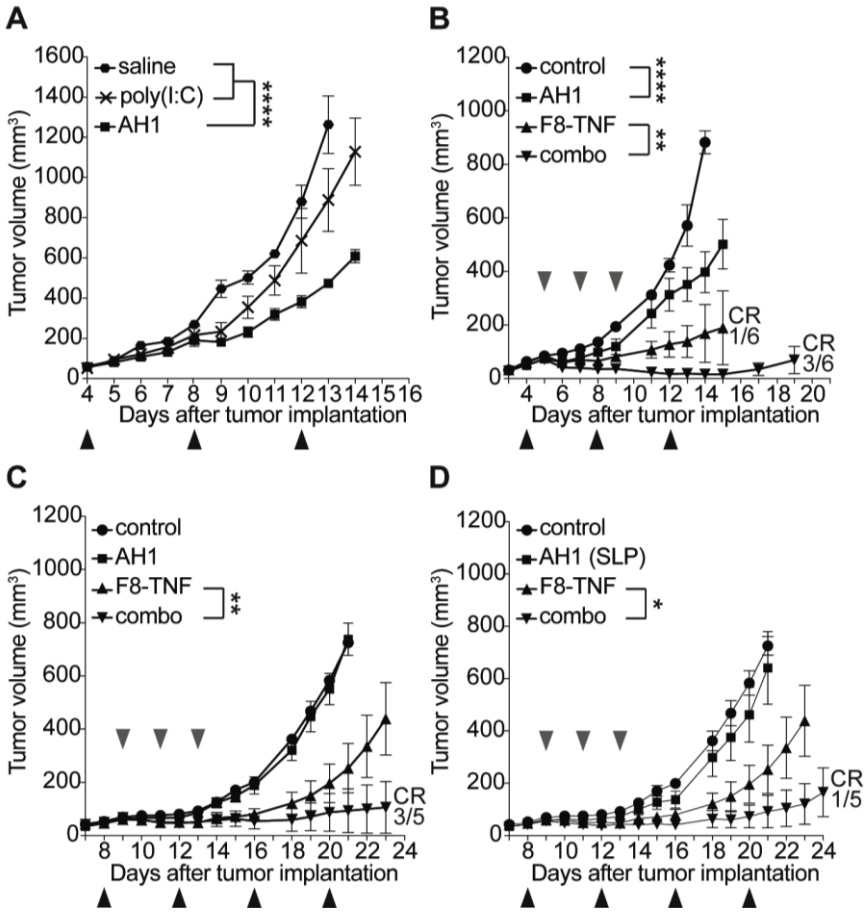

Figure 1. Therapeutic activity of AH1 vaccination in tumor-bearing mice.

A, Mice were injected with 3 x 10^6 WEHI-164 cells and treatment was started when tumors reached a size of approximately 50 mm^3. Mice were randomly grouped (n = 5) and received either the AH1 vaccine (50 µg AH1 peptide + 100 µg poly(I:C) in saline), poly(I:C) alone or saline alone subcutaneously (black arrows). ****, $p < 0.0001$ (regular two-way ANOVA test with the Bonferroni post-test). Data represent mean tumor volumes (± SEM). **B,** WEHI-164 bearing mice were treated either with the AH1 vaccine alone, 1 µg F8-TNF alone or their combination (n = 5). Poly(I:C) alone was used as negative control (n = 5). Subcutaneous vaccination was performed every 4 days (black arrows), F8-TNF was injected intravenously (grey arrows) in the lateral tail vein every 48 h, starting on the day after the first vaccination. CR = complete response. ****, $p < 0.0001$, **, $p < 0.01$ (regular two-way ANOVA test with the Bonferroni post-test). Data represent mean tumor volumes (± SEM). **C,** CT26 colon carcinoma-bearing mice were treated as de-

scribed in B, either with the AH1 vaccine alone, 2.5 µg F8-TNF alone or the combination thereof (n = 5). Poly(I:C) alone was used as negative control (n = 5). CR = complete response. **, $p < 0.01$ (regular two-way ANOVA test with the Bonferroni post-test). Data represent mean tumor volumes (± SEM). **D,** The performance of a synthetic long peptide (SLP) of the natural gp70 amino acid sequence consisting of the AH1 domain ($CD8^+$ T cell epitope) and predicted $CD4^+$ T cell epitopes was tested in CT26-bearing mice. Vaccination was performed as described in B (black arrows) and three injections of 2.5 µg of F8-TNF were given intravenously in the lateral tail vein (grey arrows). CR = complete response. *, $p < 0.05$ (regular two-way ANOVA test with the Bonferroni post-test). Data represent mean tumor volumes (± SEM).

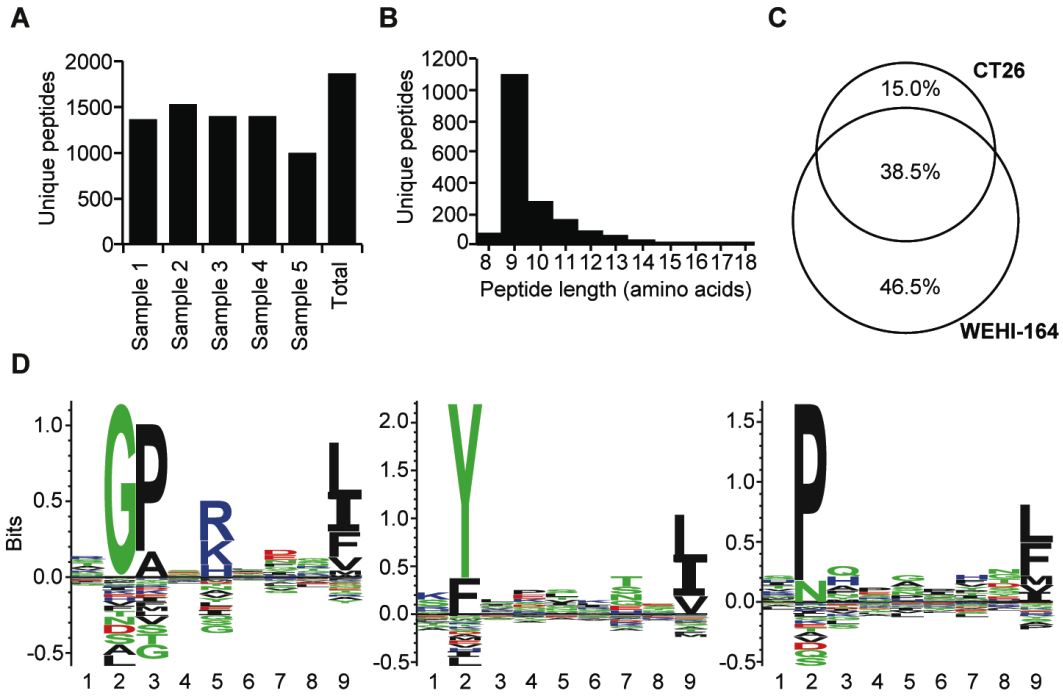

Figure 2. MHC class I peptidome analysis of CT26 cells.

A, Number of MHC class I-bound peptides identified in five independent analyses of 100 million cells. **B,** Length distribution of peptides identified from the CT26 cell line. **C,** Comparison of the MHC class I peptidome from CT26 and WEHI-164 cells. Venn diagrams were computed from the peptides identified from CT26 and WEHI-164, respectively**. D,** H-2 specific motifs from the MHC class I peptidome of CT26. All unique 9mers were subjected to Gibbs clustering with the GibbsCluster-2.0 Server (37)**.** Motifs of H-2D^{d}, -K^{d} and -L^{d} alleles from 693, 585, and 552 peptides are presented from left to right.

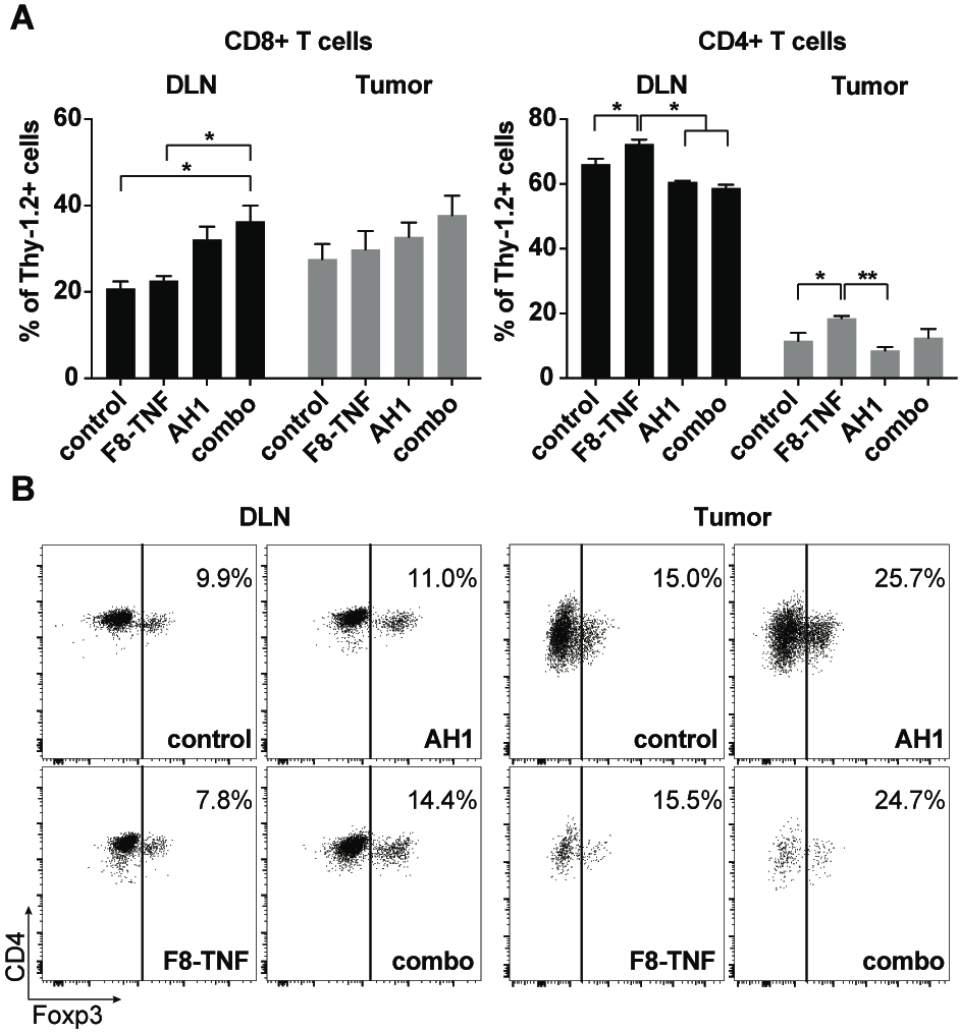

Figure 3. Flow cytometric analysis of CD8$^+$ and CD4$^+$ T cells in draining lymph nodes and tumors.

A, Comparison of CD8$^+$ T cell (left bar plot) and CD4$^+$ T cell (right bar plot) density in tumor draining lymph nodes (DLN) among the different treatment groups of CT26-bearing mice. *, $p < 0.05$, **, $p < 0.01$ (regular two-way ANOVA test with the Bonferroni post-test). Data represent mean (± SEM). n = 4 per group. **B,** Representative flow cytometric dot plots showing the expression of Foxp3 on CD4$^+$ T cells in DLN and tumors of control mice, AH1 vaccine-, F8-TNF- and combo treated mice (n = 4 per group). Numbers indicate the percentage of Foxp3$^+$ cells among total CD4$^+$ T cells.

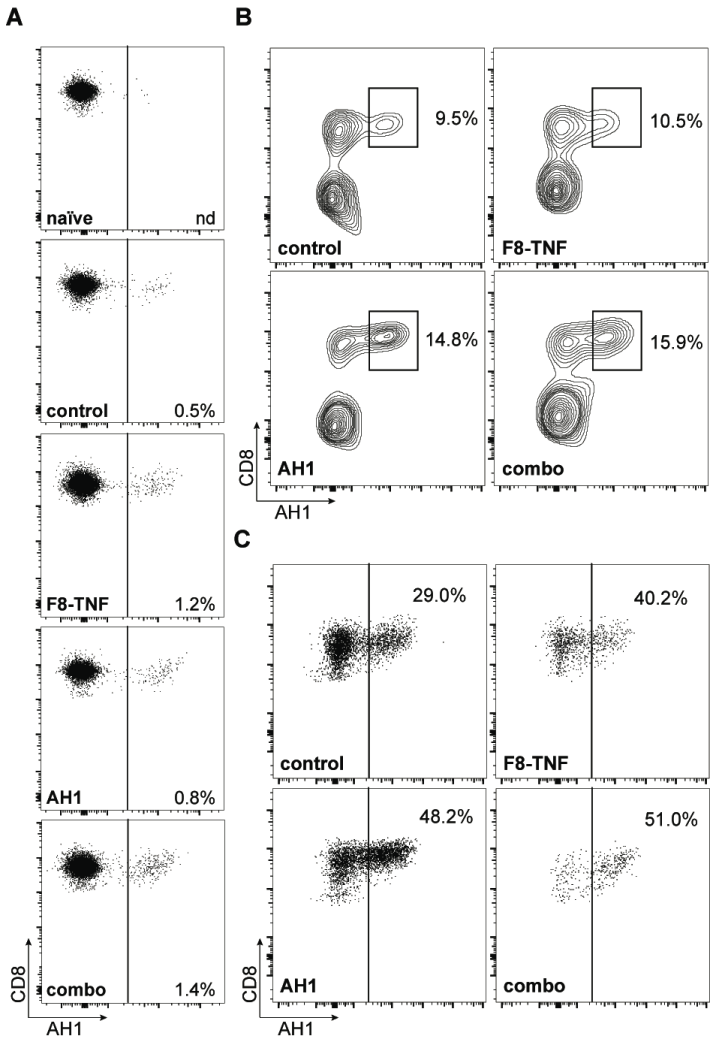

Figure 4. Analysis of AH1-specific CD8$^+$ T cells

A, Analysis of AH1-specific cells among total CD8$^+$ T cells in tumor draining lymph nodes. Numbers indicate the frequency of antigen-specific CD8$^+$ T cells (n = 4 per group). **B,** Representative flow cytometric dot plots of AH1$^+$ CD8$^+$ T cells in tumors of mice from the different treatment groups (n = 4). Plots were gated on total Thy1.2$^+$ cells and **C,** on total CD8$^+$ T cells. Numbers indicate the percentage of AH1-specific CD8$^+$ T cells.

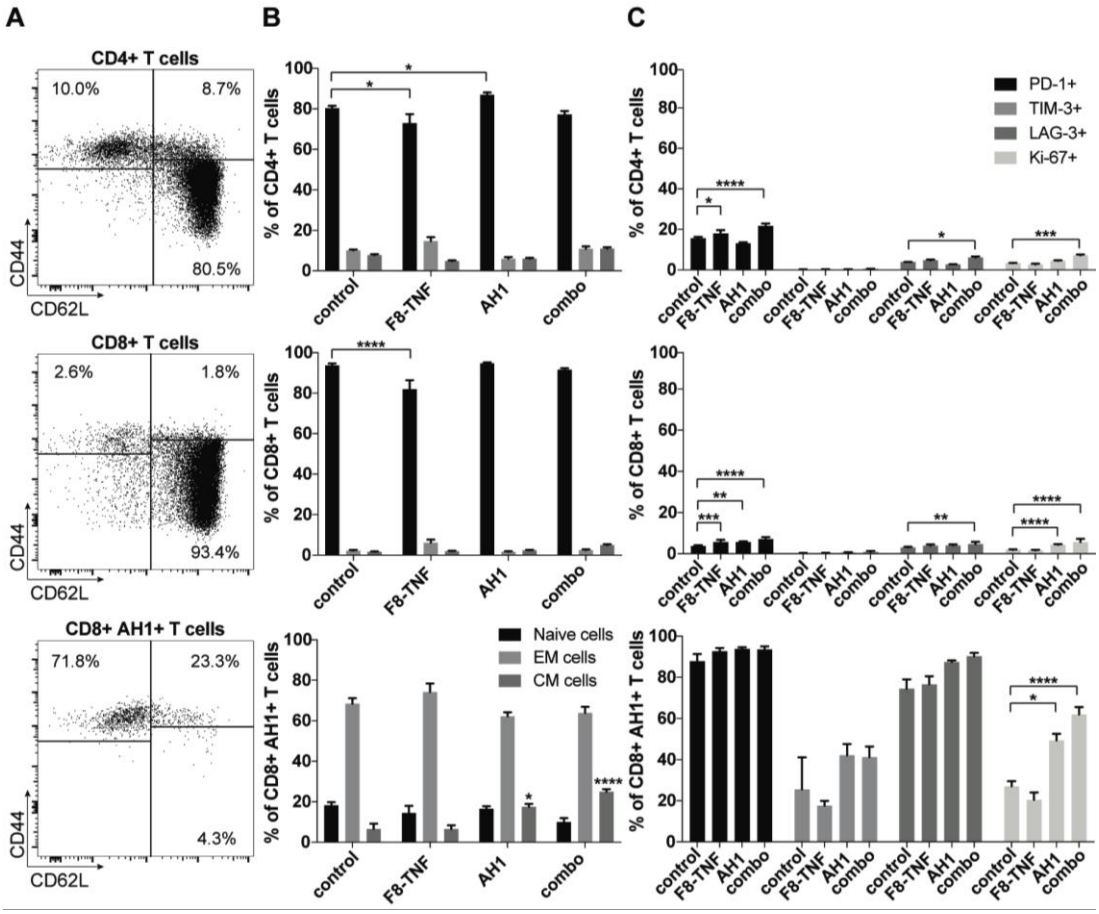

Figure 5. Phenotype analysis of CD4$^+$ T cells, CD8$^+$ T cells and AH1-specific cells in DLN

A, Representative FACS plots of CD4$^+$ T cell, CD8$^+$ T cell and AH1$^+$ CD8$^+$ T cell subsets: naïve (CD44$^-$ CD62L$^+$), central memory (CD44$^+$ CD62L$^+$) and effector memory (CD44$^+$ CD62L$^-$) phenotypes. **B,** Bar plots showing the percentage of naïve, central memory (CM) and effector memory (EM) cells among CD4$^+$ T cells, CD8$^+$ T cells and AH1$^+$ CD8$^+$ T cells in draining lymph nodes of mice from the different therapy groups (n = 4). Statistical differences were assessed between the treatment groups and control mice. *, $p < 0.05$, ****, $p < 0.0001$ (regular two-way ANOVA test with the Bonferroni post-test). Data represent mean (± SEM). **C,** Expression of exhaustion markers PD-1, TIM-3 and LAG-3, and of the proliferation marker Ki-67 was assessed among CD4$^+$ T cells, CD8$^+$ T cells and AH1$^+$ CD8$^+$ T cells in draining lymph nodes of treated mice (n = 4 per group). Statistical differences were assessed between the treatment groups and control mice. Data represent mean (± SEM). *, $p < 0.05$, **, $p < 0.01$, ***, $p < 0.001$, ****, $p < 0.0001$ (regular two-way ANOVA test with the Bonferroni post-test).

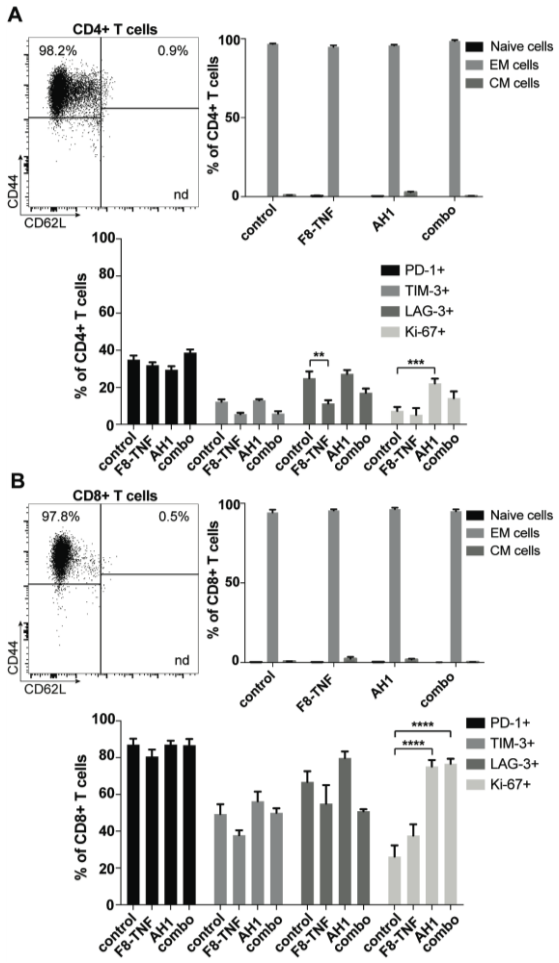

Figure 6. Phenotype analysis of CD4$^+$ T cells and CD8$^+$ T cells in tumors

A, Flow cytometric dot plot (top left) of CD4$^+$ T cell subsets in CT26 tumors: naïve (CD44$^-$ CD62L$^+$), central memory (CD44$^+$ CD62L$^+$) and effector memory (CD44$^+$ CD62L$^-$) phenotypes. A bar plot (top right) shows the percentage of naïve, central memory (CM) and effector memory (EM) cells among CD4$^+$ T cells in tumors of mice from the different therapy groups (n = 4). Expression of exhaustion markers PD-1, TIM-3 and LAG-3, and of the proliferation marker Ki-67 was assessed among tumor infiltrating CD4$^+$ T cells (bottom). Statistical differences were assessed between the treatment groups and control mice. Data represent mean (± SEM). **, $p < 0.01$, ***, $p < 0.001$ (regular two-way ANOVA test with the Bonferroni post-test). **B,** The same analysis was performed for tumor infiltrating CD8$^+$ T cells (n = 4 mice per group). Statistical differences were assessed between the treatment groups and control mice. Data represent mean (± SEM). ****, $p < 0.0001$ (regular two-way ANOVA test with the Bonferroni post-test).

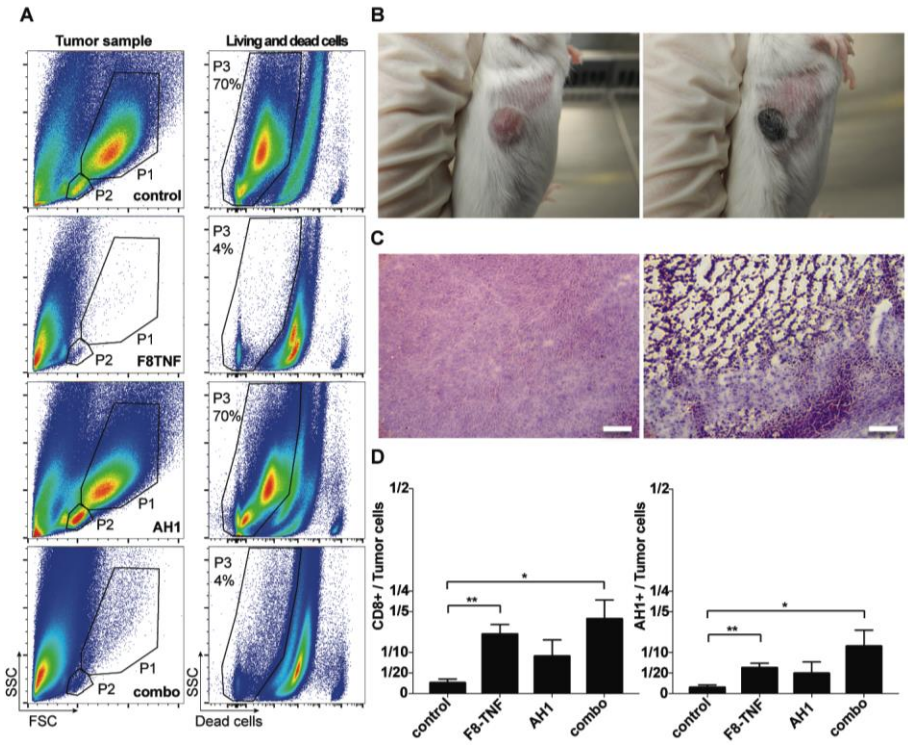

Figure 7. Hemorrhagic necrosis in tumors due to F8-TNF

A, Representative FACS plots of tumor samples from mice of the four treatment groups. Definiton of tumor cells (P1) and the T cell containing population (P2) by forward (FSC) and side scatter (SSC) characteristics (left column). P3 shows the percentage of living cells among all analyzed cells. **B,** Representative images of CT26 tumors before the start of the F8-TNF treatment (left image), and 16 h after the first injection of 2.5 µg of the immunocytokine (right image) **C,** *Ex vivo* H&E analysis on WEHI-164 tumor sections 16 hours after treatment with saline (left) or F8-TNF (right). Magnification, x10. Scale bar, 100 µm. **D,** Bar plots representing the $CD8^+$ T cell to tumor cell ratio (left plot) or the $AH1^+$ $CD8^+$ T cell to tumor ratio in treated mice (n = 4 per group) determined by flow cytometry. Statistical differences were assessed between the treatment groups and control mice. Data represent mean (± SEM). *, $p < 0.05$, **, $p < 0.01$ (unpaired, two-tailed *t* test).